NASA Technical Memorandum 104058

NASP Aeroservothermoelasticity Studies

Robert V. Doggett, Jr., Rodney H. Ricketts,
T. E. Noll, and John B. Malone

April 1991

National Aeronautics and
Space Administration

Langley Research Center
Hampton, Virginia 23665-5225

NASP Aeroservothermoelasticity Studies

By

Robert V. Doggett, Jr.; Rodney H. Ricketts; T. E. Noll; and John B. Malone

SUMMARY

Some illustrative results obtained from work accomplished under the Aerothermoelasticity work breakdown structure (WBS) element (4.7.02) of the National Aero-Space Plane (NASP) Technology Maturation Program (TMP) are presented and discussed. The objectives of the Aerothermoelasticity element were to develop analytical methods applicable to aerospace plane type configurations, to conduct analytical studies to identify potential problems and to evaluate potential solutions to said problems, and to provide an experimental data base to verify codes and analytical trends. Work accomplished in the three areas of experimental data base, unsteady aerodynamics, and integrated analysis methodology are described. Some of the specific topics discussed are transonic wind-tunnel aeroelastic model tests of cantilever delta-wing models, of an all-moveable delta-wing model, and of aileron buzz models; unsteady aerodynamic theory correlation with experiment and theory improvements; and integrated analysis methodology results for thermal effects on vibration, for thermal effects on flutter, and for improving aeroelastic performance by using active controls.

INTRODUCTION

The purpose of this paper is to present some illustrative results obtained from the Aerothermoelasticity work breakdown structure (WBS) element (4.7.02) of the National Aero-Space Plane (NASP) Technology Maturation Program (TMP). The overall purpose of the TMP was to develop further all of the many facets of advanced technology needed to ensure the successful design of an aerospace plane. The specific objectives of the Aerothermoelasticity element of the TMP were to develop, for aerothermoelasticity, analytical methods applicable to aerospace plane type configurations, to conduct analytical studies to identify potential problems and to evaluate potential solutions to said problems, and to provide an experimental data base to verify analysis codes and analytical trends.

This work emphasized three areas, namely, experimental data base, unsteady aerodynamics, and integrated analysis methodology. The experimental data base work focused on acquiring data to provide a clearer understanding of potential NASP aeroelastic problems and for validating analytical methods. The unsteady aerodynamics work focused on improving and validating advanced aerodynamics methods to meet the specific requirements of NASP applications. The integrated analysis methodology work focused on developing aeroelastic analysis methodology that incorporates the latest techniques needed to meet the specific requirements of NASP configurations and then applying these methods to assess the aeroelastic performance of generic NASP designs. Significant accomplishments have been made in each of these areas as shown by the illustrative results described herein.

Readers interested in a capsule summary of the accomplishments made under the Aerothermoelasticity WBS element are referred to Appendix A which is a narrative summary of the work that was performed and results obtained. Appendix B is a bibliography that includes all of the papers published to date under the Aerothermoelasticity WBS element. The list is arranged in chronological order. Instances where a paper is available in more than one form are noted in the citations.

AERO(SERVO)THERMOELASTICITY DEFINED

Aerothermoelasticity is a very specialized field and perhaps not too familiar to many scientists and engineers. It is, therefore, useful to discuss the term. It has become more or less standard practice to use geometric shapes in a pictorial fashion to depict aeroelasticity related phenomena. Garrick and Cunningham[1] suggested that the tetrahedron shown in figure 1 be used to depict aerothermoelasticity. The apexes A, I, E, and H of the tetrahedron represent aerodynamic force, inertia force, elastic force, and heat (thermal forces), respectively. The various subelements of

aerothermoelasticity are indicated by the edges and faces of the tetrahedron. For example, the line 1 that connects apex E with apex I represents natural vibrations which are governed by the inertia and elastic (stiffness) characteristics of a structure. The triangular plane 7 connecting the apexes A, I, and E represents dynamic aeroelasticity which is a coupling of aerodynamic, inertia, and elastic forces. Flutter is an example of such a phenomena. The triangle 7 is the Collar Triangle, named after the British scientist who was the first to use this figure to represent aeroelastic phenomena.[2] To arrive at their tetrahedron representation Garrick and Cunningham simply added a fourth apex H which expanded the Collar Triangle to a tetrahedron. The entire tetrahedron represents aerothermoelasticity.

Because aeroservoelastic (active control) methods have significant potential for improving aeroelastic performance/characteristics,[3] for example, increasing flutter speeds or improving ride quality, perhaps aerothermoelasticity is actually aero*servo*thermoelasticity (Some people may prefer the term aerothermoservoelasticity.) and another apex C for controls should be added thus making the tetrahedron some sort of hypersurface. Unfortunately, hypersurfaces are difficult to visualize. But, fortunately, there does appear to be a simpler representation. Because controls can be used to affect all the forces, either individually or collectively, it is necessary that an interconnection be provided between them. A sphere circumscribed about the tetrahedron provides such an interconnection. This representation is illustrated in figure 2. This sphere represent controls and provides the interconnections between the various forces. For example, the active control of mechanical vibrations is represented by the segment of the sphere (great circle) that connects apex I with apex E. The active control of dynamic aeroelastic phenomena (i.e. active flutter suppression) is represented by the spherical triangle connecting apexes A, I, and E that results from the projection of triangle 7 onto the surface of the sphere. The sphere 12, which rests on the plane of materials, and its contents represent the entire field of aeroservothermoelasticity.

Even though the graphical representation of aeroservothermoelasticity given in figure 2 is clearly not as simple as the Collar Triangle used to represent classical aeroelasticity, it does however provide a means to assist in visualizing the various couplings present in aeroservothermoelastic phenomena.

FLUTTER MODEL STUDIES

There is relatively little experimental flutter data in the literature for highly swept delta wings which are candidates for use in aerospace plane designs. Therefore, some experimental flutter studies were conducted at transonic speeds in the Langley Transonic Dynamics Tunnel (TDT) on three types of models. A description of the TDT is given in reference 4. Three types of models were investigated. The first type was cantilever mounted delta wings and included parametric variations in sweep angle, fraction of the root chord that was clamped, and fraction of outboard span that was removed to form clipped-delta wings. The second type was an all-moveable wing that included parametric changes in root flexibility, pitch axis location, pitch stiffness, and pitch inertia. The third type was aileron buzz models that included parametric changes in simulated actuator stiffness, wing sweep angle, and airfoil thickness. Illustrative results of these tests are discussed in the following three sections.

Delta-Wing Flutter Studies - Experiment and Theory

Experimental and analytical transonic flutter boundaries are presented in figure 3 for a 72°-swept delta-wing model that was cantilever mounted along its entire root chord. These experimental results were first published in reference 5. The theoretical results are from reference 6. The model had a 3-percent-thick biconvex airfoil section. A sketch of the model showing its geometry and construction is presented at the left in the figure. The flutter boundaries shown at the right in the figure are presented as the variation of flutter dynamic pressure with Mach number. The stable region is below the curves; the unstable region is above the curves. The experimental boundary, circle symbols, is similar to that usually observed, namely, a nearly constant value at subsonic Mach numbers then decreasing to a minimum value at transonic Mach numbers followed by a sharp increase at supersonic Mach numbers. Two sets of analytical results are shown. The dashed

line denotes the calculated boundary obtained by using linear kernel function unsteady aerodynamic theory.[7] At subsonic speeds the calculated results are conservative with respect to the experimental data, whereas at supersonic speeds they are slightly unconservative with respect to the experimental results. The analytical results obtained by using the nonlinear CAP-TSD[8] procedure, denoted by the solid line, are in excellent agreement with the experimental results throughout the Mach number range studied. Furthermore, the CAP-TSD results are slightly conservative with respect to the experimental results, which is a desirable situation.

All-Moveable Delta-Wing Aeroelastic Studies

All-moveable delta-wing configurations are candidates for use in aerospace plane applications. Therefore, some wind-tunnel studies were conducted using a 72°-swept delta-wing model that was mounted to a flexure which allowed variations in pitch and plunge stiffness as well as variations in mass and mass unbalance. The variable stiffness provision allowed simulation of actuator and fuselage attachment flexibilities. A photograph of the model is shown at the upper left in figure 4. A sketch of the model and the flexible support system is shown at the upper right. The experimental flutter boundary for the pivot point at 37.5 percent of the mean aerodynamic chord (MAC) is indicated by circle symbols at the lower left in the figure as the variation of flutter dynamic pressure with Mach number. Also shown in the figure are analytical flutter results (square symbols), that were obtained by using kernel function unsteady aerodynamics.[7] The experimental and analytical flutter boundaries are in good agreement. One static divergence condition was obtained for the pivot at 0.60 percent of the MAC. The divergence results are shown at the lower right in the figure where both experimental and analytical results are presented. Again, the theoretical result is in good agreement with the experimental value. Some additional details relative to this study are presented in reference 9.

Aileron Buzz Studies

An aerospace plane may incorporate large trailing-edge control surfaces that may experience a phenomena known as aileron buzz. Aileron buzz is a single-degree-of-freedom oscillation of the control surface about its hinge line that occurs at transonic speeds. Some wind-tunnel model studies were conducted using 60°-swept and 72°-swept delta-wing models that were equipped with full-span trailing-edge control surfaces. Some results from these studies are presented in references 10 and 11. The results included herein in figure 5 are from reference 11. The 60°- and 72°-swept models were tested for two airfoil thickness-to-chord ratios, namely, 3 percent and 6 percent. Provision was provided for changing the attachment flexibility of the control surfaces to determine the effects of simulated actuator stiffness. A photograph of one of the models mounted in the TDT is shown at the top in the figure. The geometry of the models is shown by the sketches at the lower left. Some buzz data obtained for these models are shown at the lower right in the figure as the variation of dynamic pressure with Mach number. Control surface buzz occurred for all four models near a Mach number of one. Buzz onset Mach number was lower for the 60°-swept model than it was for the 72°-swept model. Furthermore, for a given sweep angle, the configuration with the thinner airfoil section had the lower buzz onset Mach number. For the 60°-swept model with the thin airfoil section a wing-bending control-surface-rotation flutter was observed. This phenomenon was not observed for the other configurations. Although not shown here, some additional buzz results were obtained for a 60°-swept configuration for variations in stimulated actuator stiffness. These results showed that buzz onset Mach number increased with increasing stiffness, and that the amplitudes of the buzz oscillations became more violent as M=1.0 was approached.

ENGINE INLET LIP AEROELASTIC ANALYSIS

Preliminary assessments indicated a potential for aeroelastic instabilities of a scramjet engine inlet lip. Therefore, an aeroelastic analysis was conducted of a generic design that is representative of those being considered for aerospace plane applications. A sketch of the engine lip arrangement is shown in the sketch at the left in figure 6. An equivalent-plate finite-element model developed

using EAL[14] was used to represent the built-up structure of the full-scale design. Added mass was included to represent active cooling requirements. Aeroelastic analyses were performed using kernel function unsteady aerodynamic theory[7] over the Mach number range from 0.6 to 2.0. Analyses were conducted using piston theory[12] over the Mach number range from 1.2 to 2.5. Two piston theory analyses were made, one without thickness effects included and one with thickness effects included. Results of the analyses, shown to the right in the figure as the variation of dynamic pressure with Mach number, indicate that static divergence of the lip is the critical aeroelastic instability. The lowest instability boundary is given by the kernel function results. The predicted instability condition, however, is outside the flight envelope for the generic design considered here.

UNSTEADY AERODYNAMIC THEORY IMPROVEMENTS

As shown previously, existing unsteady transonic aeroelastic codes such as CAP-TSD[8] can be used to predict accurately the transonic flutter characteristics of low-aspect-ratio delta wings. However, the accurate prediction of the flutter characteristics of complete NASP-like configurations will require advances over existing methods. The linearized surface boundary conditions using cartesian grids as included in CAP-TSD are not satisfactory for application to the highly blended wing/fuselage, large fineness ratio configurations with swept, tapered vertical fins which are being considered for aerospace plane configurations. To model accurately the important aerodynamic interaction effects that occur on such configurations, computation methods that use body-fitted grids are required. Consequently, work has begun on developing a new full-potential-flow equation (FPE) method that is based on a finite-volume formulation using body-fitted grids. Prior to developing the three dimensional method a two-dimensional formulation was implemented and some sample results obtained for purposes of evaluation. Some illustrative results are shown in figure 7 for a lifting airfoil at transonic speeds. The body-fitted grid used is shown on the left in the figure. On the right is the calculated distribution of the pressure coefficient along the airfoil chord for the airfoil at 2° angle-of-attack at M=0.75. A comparison of the FPE results, indicated by the solid line, with the more exact Euler results (circle symbols) are excellent. Experience gained during the development and use of the two-dimensional method will provide the foundation upon which to build the three-dimensional capability in the future.

THERMAL EFFECTS INTO FINITE-ELEMENT ANALYSIS

At very high speeds thermal effects can have adverse effects on structural stiffness. It is important, therefore, that such effects be included in analysis capability to ensure accurate predictions of aeroelastic characteristics. Heating may affect structural stiffness in several ways. Elevated temperatures may reduce material moduli and thermal gradients may produce internal stresses that result in stiffness changes. A method for integrating thermal effects into finite-element analysis is presented in reference 13. The block diagram shown in figure 8 depicts the steps necessary for developing a structural stiffness matrix that includes the effects of elevated temperature on material properties and the effects of internal stresses produced by temperature gradients. The process begins with a "cold" mathematical model. This cold model is modified to account for changes in material properties that are produced by heating effects that occur at the flight condition being analyzed. The second step determines the prestress in the structure that results from temperature gradients. As shown in the figure the second phase of the process follows one of two paths depending on whether the structure is isotropic or composite (anisotropic). Finally, the stiffness matrix is modified to account for the effects of the prestress. Therefore, the final model includes the effects on stiffness of both elevated temperature and thermal gradients. This modified stiffness matrix may now be used in an aeroelastic analysis so that the effects of heating are accounted for. This technique has been integrated into the EAL[14] finite-element analysis code. Some results obtained from the application of this method are presented in the following two sections.

Thermal Effects on Structural Vibration Frequencies

Conley and Spain, as indicated in reference 15, pp. 48 and 49, have recently conducted some experimental and analytical studies to determine the effects of heating on an aluminum wing-box model comprised of spars, ribs, and curved skin panels. Their analysis was accomplished using the finite-element procedure discussed in the preceding section. A photograph of the test specimen that they used is shown in the photograph at the upper left in figure 9. This model was instrumented with accelerometers to measure dynamic response and thermocouples to measure temperature distribution. The natural frequencies of the test article were measured while it was heated up and while it was allowed to cool down to ambient temperature. Shown on the lower left in the figure are contours of constant temperature obtained for the hottest condition. These data were obtained by using surface spline techniques to interpolate the temperature readings obtained from the array of thermocouples mounted on the structure. As these contours indicate there were significant temperature gradients. Shown on the right is the variation of natural frequency for the first four natural modes as the specimen was heated up and then allowed to cool down. The experimental frequencies are indicated by the open symbols. Analytical results obtained by using the previously described finite-element analysis method that incorporated the effects on stiffness of elevated temperature and internal stress resulting for temperature gradients compare reasonably well with the experimental results. These data clearly indicate that the effects of temperature on the natural frequencies of a built-up structure may be quite complicated and can result in either stiffness decreases or stiffness increases.

Correlation of Finite-Element Analysis with Previous Flutter Experiment

There is not much experimental data available in the literature on the effects of elevated temperature on structural dynamics. Runyan and Jones[16], however, did publish some results of a flutter experiment in which a solid aluminium wing fluttered due to transient heating effects. The model was placed in a Mach number equal 2.0 air jet that was heated to 800°F. The model was observed to flutter 2 seconds after the flow commenced. A photograph of the cantilever-mounted model in the air jet is shown on the left in figure 10.

The finite-element analysis method described previously was applied to this experiment. First, the effects on the stiffness of the model were calculated. These results are shown on the upper right in the figure where the ratio of the torsional stiffness (GJ) of the hot model is ratioed to the GJ of the cold model. Results are presented that show the effects of property change only, prestress only, and combined property and prestress. Note that prestress is considerably more effective in reducing the structural stiffness than are the changes in material properties. To the left of the present results are results given by Runyan and Jones. The present results, which represent average reductions in stiffness, should be compared with the previous results labeled "MID." This comparison is good. The hot stiffness model was used in a flutter analysis that used piston theory unsteady aerodynamics.[12] The flutter analysis was conducted using the STABCAR[17] aeroelastic stability code. The calculated flutter dynamic pressure of 7445 lb/ft^2 is within eight percent of the experimental value of 6895 lb/ft^2. Although additional experimental results are needed to validate fully this finite-element analysis method, these results do give confidence to using the method in flutter applications.

AEROELASTIC ANALYSIS OF A GENERIC NASP DESIGN

To assist in understanding better the aeroelastic characteristics of NASP-like vehicles some flutter and ride quality (gust response) analyses were conducted for generic NASP designs.[13,18,20,21] These studies included the analysis of hot and cold vehicles and in some instances the use of active controls to improve aeroelastic performance. Some illustrative results from these studies are presented in the following two sections.

Aerodynamic Heating Effects on Flutter

The previously mentioned finite-element analysis method with aerodynamic heating effects included was applied to a generic aerospace plane design to assess the effects of heating on flutter.

Some results of this study taken from reference 13 are presented here in figure 11. A sketch of the configuration studied is shown at the top in the figure. Two structural configurations were studied. For one, the structure was assumed to be made of titanium-aluminide (baseline configuration); for the other, the structure was assumed to be made of carbon-carbon. The temperature distributions were based on radiation equilibrium temperatures obtained by using the method described by Sova and Divan.[19]

Some effects of aerodynamic heating on structural stiffness can be assessed by examining the calculated frequencies for the baseline and carbon-carbon models shown on the left in the figure. These data are for M=6. Three sets of frequencies are presented: the first for the cold, unheated condition; the second where only the temperature effects on material properties are considered; and the third where both the effects of property change and internal thermal stresses are included. It is interesting to note that for this case the frequencies were reduced by changes in material properties (decrease in stiffness), but were increased by thermal stress effects (increase in stiffness). Although the natural frequencies were changed by heating effects, the mode shapes essentially remained unchanged.

Some calculated flutter results in the form of the variation of flutter dynamic pressure with Mach number are shown at the lower right in the figure. The solid circle symbols are the boundary for the cold baseline configuration. The flutter mechanism was primarily a coupling of the second and third natural vibration modes, the fundamental wing-bending mode and a highly coupled wing-bending/second fuselage-bending mode, respectively. Generally speaking, the flutter dynamic pressure was decreased by including aerodynamic heating effects on structural stiffness. The greater reduction occurred for the hot baseline configuration. At M=4 the flutter dynamic pressure for the hot carbon-carbon configuration was the same as for the cold baseline (no effect of heating). At the higher Mach numbers the flutter dynamic pressure is lower. This is probably due to a change in the flutter mechanism from the previously mentioned coupling to a coupling of the third and fourth natural vibration modes. The primary component of the fourth mode is wing torsion. It is not uncommon for changes in modal coupling to cause sharp changes in flutter boundaries as observed here.

Active Control of Aeroelastic Response

As indicated in the preceding discussion the flutter dynamic pressure of a generic aerospace plane configuration can be significantly reduced by aerodynamic heating effects. Because active control concepts have been shown to be effective in increasing flutter speeds and improving other types of aeroelastic response as well,[3] some advance aeroservoelastic analysis methods were applied to a generic configuration.[20,21] Two concepts were studied, flutter suppression and ride quality control (gust load alleviation). A sketch of the configuration studied is shown at the top of the figure. At the bottom right in the figure are some flutter results in terms of the ratio of the flutter dynamic pressure q for a hot vehicle to the flutter dynamic pressure of the vehicle cold ($q_{f_{cold}}$) for M=2 and 4. Aerodynamic heating reduces the flutter dynamic pressure at both Mach numbers as evidenced by the top of the cross-hatched bars being at values of the ratio less than one. For the M=2 hot vehicle predictions, a deceleration from M=4 was assumed such that the heat loads at M=4 were used for the M=2 calculations. The tops of the shaded bars indicated flutter dynamic pressure that is attained by using active controls. The top of the shaded bar for M=2 represents a sea level condition. Presented at the lower left in the figure are some ride quality results as measured by normal acceleration at the pilot's station. These results are for a cold configuration at M=4. Results for the hot configurations were similar. The sharp peaks associated with response in elastic modes of the vehicle are sharply attenuated by the use of the active ride control system.

CONCLUDING REMARKS

Some illustrative results obtained from work accomplished under the Aerothermoelasticity work breakdown structure (WBS) element of the National Aero-Space Plane (NASP) Technology Maturation Program (TMP) have been presented and discussed. The objectives of the Aerothermoelasticity element were to develop analytical methods applicable to aerospace plane type configurations, to conduct analytical studies to identify potential problems and to evaluate potential solu-

tions to said problems, and to provide an experimental data base to verify codes and analytical trends.

The work described emphasized three areas, namely, experimental data base, unsteady aerodynamics, and integrated analysis methodology. Some of the specific topics discussed are listed on the figure. The experimental data base work focused on obtaining data for either acquiring a clearer understanding of potential NASP aeroelastic problems or for acquiring a basis for validating analytical methods. Most of the experimental work was transonic wind-tunnel aeroelastic model tests. The unsteady aerodynamics work focused on improving and validating advanced aerodynamics methods to meet the specific requirements of NASP applications. The integrated analysis methodology work focused on developing aeroelastic analysis methodology that incorporates the latest techniques needed to meet the specific requirements of NASP configurations and then applying these methods to assess the aeroelastic performance of generic NASP designs.

REFERENCES

1. Garrick, I. E.; and Cunningham, H. J.: Problems and Developments in Aerothermoelasticity. Proceeding of Symposium on Aerothermoelasticity, ASD-TR-61-6435, Feb. 1962.
2. Collar, A. R.: The Expending Domain of Aeroelasticity. Journal of the Royal Aeronautical Society, Vol. 50, pp. 613-636, Aug. 1946.
3. Noll, T. E.: Aeroservoelasticity. Presented at the AIAA/ASME/ASCE/AHS/ASC 31st Structures, Structural Dynamics, and Materials Conference, AIAA Paper 90-1073, Apr. 1990. (Also available as NASA TM 102620, Mar. 1990.)
4. Reed, W. H., III.: Aeroelasticity Matters: Some Reflections of Two Decades of Testing in the NASA Langley Transonic Dynamics Tunnel. Collected Papers of International Symposium on Aeroelasticity, DGLR-Bericht 82-01, pp. 105-120, Oct. 1981.
5. Doggett, Robert V., Jr.; Soistmann, David L.; Spain, Charles V.; Parker, Ellen C.; and Silva, Walter A.: Some Experimental Transonic Flutter Characteristics of Two 72°-Sweep Delta-Wing Models. NASP TM-1079, Aug. 1989. (A slightly expanded version of this paper is available as Experimental Transonic Flutter Characteristics of Two 72°-Sweep Delta-Wing Models, NASA TM-101659, Nov. 1989.)
6. Soistmann, David L.; and Gibbons, Michael D.: Some Analytical Transonic Flutter Characteristics of a Highly Swept Delta Wing. Presented at Seventh National Aero-Space Plane Technology Symposium, Paper No. 63, Oct. 1989. (Available as NASP CR-1084, May 1990.)
7. Cunningham, A. M., Jr.: A Steady and Oscillatory Kernel Function Method for Interfering Surfaces in Subsonic, Transonic, and Supersonic Flow. NASA CR-144895, 1976.
8. Batina, J. T.; Seidel, D. A.; Bland, S. R.; and Bennett, R. M: Unsteady Transonic Flow Calculations for Realistic Aircraft Configurations. J. of Aircraft, Vol. 26. No. 1, pp. 21-28, 1989. (An earlier version of this paper is available as NASA TM 89120, 1987.)
9. Spain, C. V.; Soistmann, D. L.; Parker, E. C.; Gibbons, M. D.; Gilbert, M. G.: An Overview of Selected NASP Aeroelastic Studies at NASA Langley Research Center. Presented at the AIAA Second International Aerospace Planes Conference, AIAA Paper 90-5218, Oct. 1990.
10. Parker, Ellen C.; Spain, Charles V.; and Soistmann, David L.: Experimental Transonic Buzz Characteristics of a Clipped-Delta-Wing Model with a Full-Span Aileron. NASP CR-1083, May 1990.
11. Parker, Ellen C.; Spain, Charles V.; and Soistmann, David L.: Aileron Buzz Investigated on Several Generic NASP Wing Configurations. Presented at AIAA/ASME/ASCE/AHS/ASC 32nd Structures, Structural Dynamics, and Materials Conference, AIAA Paper 91-0936, Apr.1991.
12. Morgan, H. G.; Huckel, V.; and Runyan, H. L.: Procedure for Calculating Flutter at High Supersonic Speeds Including Camber Deflections, and Comparison With Experimental Results. NACA TN 4335, 1958.
13. Spain, C. V.; Soistmann, D. L.; and Linville, T. W.: Integration of Thermal Effects Into Finite Element Aerothermoelastic Analysis with Illustrative Results. Presented at Sixth National

Aero-Space Plane Technology Symposium, Paper No. 9, Apr. 1989. (Available as NASP CR-1059, Aug. 1989.)
14. Whetstone, W.: EISI-EAL Engineering Analysis Language Reference Manual. Engineering Information Systems, Inc., San Jose, CA, 1983.
15. Wynne, Eleanor C.: Structural Dynamics Division Research and Technology Accomplishments for F.Y. 1990 and Plans for F.Y. 1991. NASA TM 102770, Jan. 1991.
16. Runyan, Harry L.; and Jones, Nan H.: Effect of Aerodynamic Heating on the Flutter of a Rectangular Wing at a Mach Number of 2. NASA TN D-460, 1960.
17. Adams, W. M., Jr.; Tiffany, S. H.; Newsom, J. R.; and Peele, E. L.: STABCAR-A Program for Finding Characteristic Roots of Systems Having Transcendental Stability Matrices. NASA TP-2165, 1984.
18. Heeg, J.; Gilbert, M. G.; and Pototzky, A. S.: Static and Dynamic Aeroelastic Characterization of an Aerodynamically-Heated Generic Hypersonic Aircraft Configuration. Presented at AIAA/ASME/ASCE/ AHS/ASC 31st Structures, Structural Dynamics, and Materials Conference, Work-in-Progress Session, Apr. 1990. (Available in NASA CP-3064, 1990.)
19. Sova, G.; and Divan, P.: Aerodynamic Preliminary Analysis System II, Part II User's Manual. NASA CR-182077, April 1991.
20. Gilbert, Michael G.; Heeg, Jennifer; Pototzky, Anthony S.; Spain, Charles V.; Soistmann, David L.; and Dunn, H. J.: The Application of Active Controls Technology to a Generic Hypersonic Aircraft Configuration. Presented at Seventh National Aero-Space Plane Technology Symposium, Paper No. 62, Oct. 1989. (Also available as NASA TM-101689, Jan. 1990, and as NASP TM-1097, May 1990.)
21. Heeg, J.; Gilbert, M. G.; and Pototzky, A. S.: Active Control of Aerothermoelastic Effects for a Conceptual Hypersonic Aircraft. Presented at AIAA Guidance, Navigation and Controls Conference, AIAA Paper 90-3337, Aug. 1990.

APPENDIX A
SUMMARY OF ACCOMPLISHMENTS

A narrative summary of the work conducted during the NASP Technology Maturation Program under under Aerothermoelasticity work breakdown structure element (4.7.02) is presented in this appendix.

The aerothermoelasticity effort focused on three areas, namely, experimental data base, unsteady aerodynamics, and integrated analysis methodology. Work in the experimental data base area focused on acquiring data for either acquiring a clearer understanding of potential NASP aeroelastic problems or for acquiring a basis for validating analytical methods. The work in unsteady aerodynamics area focused on improving and validating advanced aerodynamics methods to meet the specific requirements of NASP applications. The work in the integrated analysis methodology area focused on developing aeroelastic analysis methodology that incorporates the latest techniques needed to meet the specific requirements of NASP configurations and then applying these methods to assess the aeroelastic performance of generic NASP designs. Significant accomplishments have been made in each of these areas and some illustrative examples are described here.

Initial studies were made to assess the general understanding of the aeroelastic characteristics of vehicles of the type being considered for the National Aero-Space Plane. This assessment included in-house analytical studies of a generic government design and contractor studies based on historical reviews of previous work. This work clearly indicated a general deficiency in the information available with respect to the aeroelastic characteristics of NASP-like configurations, specifically, the lack of experimental flutter data on highly swept low-aspect-ratio wings and the correlation of such experimental data with analytical predictions made using advanced unsteady aerodynamic theories in the computational fluid dynamics (CFD) category. Accordingly wind-tunnel flutter-model studies were conducted in the Langley Transonic Dynamics Tunnel (TDT) to provide the additional data needed. Tests were conducted using several series of cantilever-mounted delta-wing models, an all-moveable delta-wing model, and an aileron buzz model that consisted of a delta wing with a full-span trailing-edge control surface. The cantilever-model studies clearly defined the flutter characteristics of several delta-wing configurations at subsonic and transonic speeds. The results obtained by using the all-moveable-wing model showed that either flutter or divergence could be the critical aeroelastic phenomena depending on such things as pitch axis location. The aileron buzz data obtained at transonic speeds provided buzz boundaries for different values of simulated actuator stiffness, airfoil thickness, and wing leading edge sweep.

The implementation of transonic small disturbance (TSD) theory in the CAP-TSD computer code was improved to predict more accurately and efficiently the unsteady aerodynamic characteristics of low-aspect-ratio delta-wing configurations in the nonlinear transonic speed regime. The correlation of flutter results obtained by using the CAP-TSD code with the experimental results obtained for the delta-wing-model tests was very good throughout the transonic speed range, including in the vicinity of the transonic dip or bucket. Thus, these correlations clearly established that the flutter characteristics of highly swept delta-wing configurations can be accurately predicted in the nonlinear transonic speed regime by using the CAP-TSD code.

In response to an expressed concern by engine manufacturers about possible aeroelastic instabilities of the engine inlet lip, an analysis method was developed to further analyze this potential problem. Analytical results obtained by applying the analysis method to a configuration representative of potential designs showed that aeroelastic divergence was the critical aeroelastic problem and needs to be considered in specific full-scale designs.

To facilitate the aeroelastic analysis of NASP configurations a rational means for integrating thermal effects into finite-element analysis methods was developed, implemented and validated by correlation with existing experimental data. Applications of this analysis indicate that degradation of structural stiffness properties because of thermal gradients (a prestress effect) may be larger than the degradation resulting from reductions in moduli due to elevated temperature. Flutter analysis of a generic NASP structural design indicated that aerodynamic heating effects on structural stiffness

can produce relatively large decreases in supersonic flutter speeds as compared to the flutter speeds of a "cold" configuration.

Aeroelastic analysis capability was further improved by incorporating the capability of applying advanced active control concepts to improve the aeroelastic performance of NASP vehicles. Multi-input/multi-output control concepts for ride quality improvement (gust load alleviation) and flutter suppression were evaluated for a generic NASP design by using this improved analysis capability. The results obtained indicate that ride quality (response to gusts) can be substantially improved by the use of active controls. Perhaps more importantly, the results showed that decreases in flutter speed produced by aerodynamic heating can be more than recovered by the use of active controls.

APPENDIX B
BIBLIOGRAPHY

This bibliography is a list of the publications that document the results obtained under the Aerothermoelasticity WBS element. The list is arranged in chronological order. Instances where a paper is available in more than one form are noted in the citations.

1. Newsom, Jerry R.: Aeroservoelasticity Studies for NASP. Presented at First National Aero-Space Plane Technology Symposium, Paper No. 116, May 1986.
2. Ricketts, Rodney H.; Cerro, Jeffrey A.; and Spain, Charles V.: Aeroelastic Considerations for an Airbreathing Single-Stage-To-Orbit Vehicle. Presented at Third National Aero-Space Plane Technology Symposium, Paper No. 72, June 1987,
3. Reed, Wilmer H. III; Hanson, Perry W.; and Alford, W. J., Jr.: Assessment of Flutter Model Testing Relating to the National Aero-Space Plane. NASP CR-1002, July 1987.
4. Friedman, Inger P.; Vosteen, Louis F.; Cooper, Michael J.; Gold, Ronald R.; and Reed, Wilmer H., III: Assessment of Thermoelastic Analysis and Testing Applicable to the National Aero-Space Plane. NASP CR-1017, July 1988.
5. Gibbons, M. D.; Soistmann, D. L.; Bennett, R. M.: Flutter Analysis of Highly Swept Delta Wings by Conventional Methods. Presented at 4th National Aero-Space Plane Symposium, Paper No. 67, Feb 1988. (Also available as NASA TM 101530, Nov. 1988.)
6. Pototzky A. S.; Spain, C. V.; Soistmann, D. L.; and Noll, T. E.: Application of Unsteady Aeroelastic Analysis Techniques on the National Aerospace Plane. Presented at 4th National Aero-Space Plane Symposium, Paper No. 68, Feb 1988. (Also available as NASA TM 100648, Sep. 1988.)
7. Spain, C. V.; Soistmann, D. L.; and Linville, T. W.: Integration of Thermal Effects Into Finite Element Aerothermoelastic Analysis with Illustrative Results. Presented at Sixth National Aero-Space Plane Technology Symposium, Paper No. 9, Apr. 1989. (Available as NASP CR-1059, Aug. 1989.)
8. Doggett, Robert V., Jr.; and Soistmann, David L.: Some Low-Speed Flutter Characteristics of Simple Low-Aspect-Ratio Delta Wing Models. Presented at AIAA/ASME/ASCE/AHS/ ASC 30th Structures, Structural Dynamics, and Materials Conference, AIAA Paper 89-1325, Apr. 1989. (Also available as NASA TM 101547, Jan. 1989.)
9. Gibbons, M. D.; and Batina, J. T.: Supersonic Far-Field Boundary Conditions for Transonic Small-Disturbance Theory. Presented at AIAA/ ASME/ ASCE/AHS/ASC 30th Structures, Structural Dynamics, and Materials Conference, AIAA Paper 89-1283, Apr. 1989. (Revised version, same title and authors, published in J. of Aircraft, Vol. 27, No. 9, pp. 764-70, Sep. 1990.)
10. Gold, Ronald R.; and Reed, Wilmer H. III: Design of Thermoelastic Experiments Applicable to the National Aero-Space Plane. NASP CR-1056, Aug. 1989.
11. Doggett, Robert V., Jr.; Soistmann, David L.; Spain, Charles V.; Parker, Ellen C.; and Silva, Walter A.: Some Experimental Transonic Flutter Characteristics of Two 72°-Sweep Delta-Wing Models. NASP TM-1079, Aug. 1989. (A slightly expanded version of this paper is available as Experimental Transonic Flutter Characteristics of Two 72°-Sweep Delta-Wing Models, NASA TM-101659, Nov. 1989.)
12. Gilbert, Michael G.; Heeg, Jennifer; Pototzky, Anthony S.; Spain, Charles V.; Soistmann, David L.; and Dunn, H. J.: The Application of Active Controls Technology to a Generic Hypersonic Aircraft Configuration. Presented at Seventh National Aero-Space Plane Technology Symposium, Paper No. 62, Oct. 1989. (Also available as NASA TM-101689, Jan. 1990, and as NASP TM-1097, May 1990.)
13. Soistmann, David L.; and Gibbons, Michael D.: Some Analytical Transonic Flutter Characteristics of a Highly Swept Delta Wing. Presented at Seventh National Aero-Space Plane Technology Symposium, Paper No. 63, Oct. 1989. (Available as NASP CR-1084, May 1990.)

14. Heeg, J.; Gilbert, M. G.; and Pototzky, A. S.: Static and Dynamic Aeroelastic Characterization of an Aerodynamically-Heated Generic Hypersonic Aircraft Configuration. Presented at AIAA/ASME/ASCE/ AHS/ASC 31st Structures, Structural Dynamics, and Materials Conference, Work-in-Progress Session, Apr. 1990. (Available in NASA CP-3064, 1990.)
15. Parker, Ellen C.; Spain, Charles V.; and Soistmann, David L.: Experimental Transonic Buzz Characteristics of a Clipped-Delta-Wing Model with a Full-Span Aileron. NASP CR-1083, May 1990.
16. Heeg, J.; Gilbert, M. G.; and Pototzky, A. S.: Active Control of Aerothermoelastic Effects for a Conceptual Hypersonic Aircraft. Presented at AIAA Guidance, Navigation and Controls Conference, AIAA Paper 90-3337, Aug. 1990.
17. Spain, C. V.; Soistmann, D. L.; Parker, E. C.; Gibbons, M. D.; Gilbert, M. G.: An Overview of Selected NASP Aeroelastic Studies at NASA Langley Research Center. Presented at the AIAA Second International Aerospace Planes Conference, AIAA Paper 90-5218, Oct. 1990.
18. Parker, Ellen C.; Spain, Charles V.; and Soistmann, David L.: Aileron Buzz Investigated on Several Generic NASP Wing Configurations. Presented at AIAA/ASME/ASCE/AHS/ ASC 32nd Structures, Structural Dynamics, and Materials Conference, AIAA Paper 91-0936, Apr.1991.
19. Noll, T. E.; Doggett, Robert V., Jr.; Ricketts, Rodney H.; and Malone, John B.: Aeroservothermoelasticity - A Review. Presented at Tenth National Aero-Space Plane Technology Symposium, Paper No. 104, Apr. 1991.

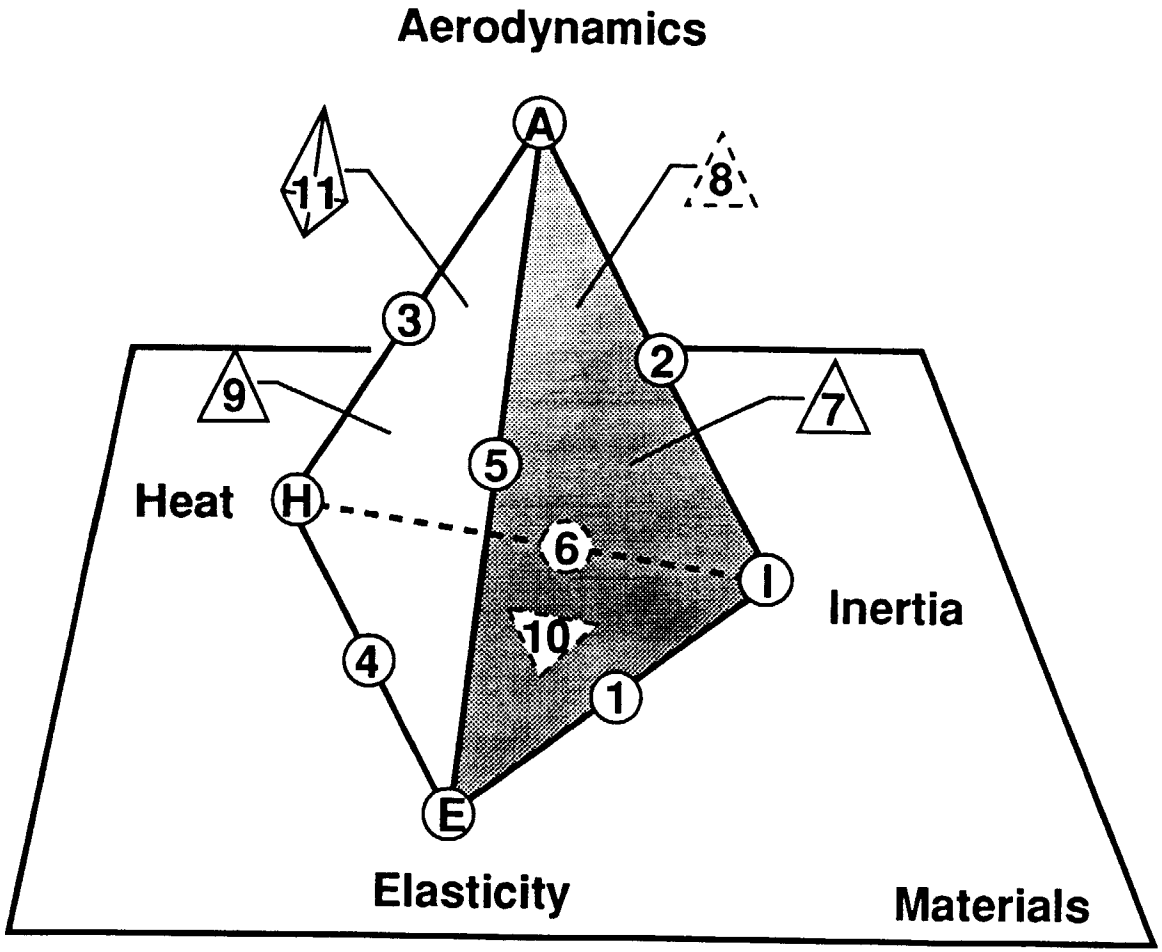

1 Vibration
2 Stability
3 Aerothermodynamics
4 Thermoelasticity
5 Aeroelasticity, static
6 Thermal molecular processes
7 Aeroelasticity, dynamic
8 Stability and heat
9 Aerothermoelasticity, static
10 Vibration and heat
11 Aerothermoelasticity, dynamic

Figure 1. - Aerothermoelasticity tetrahedron.

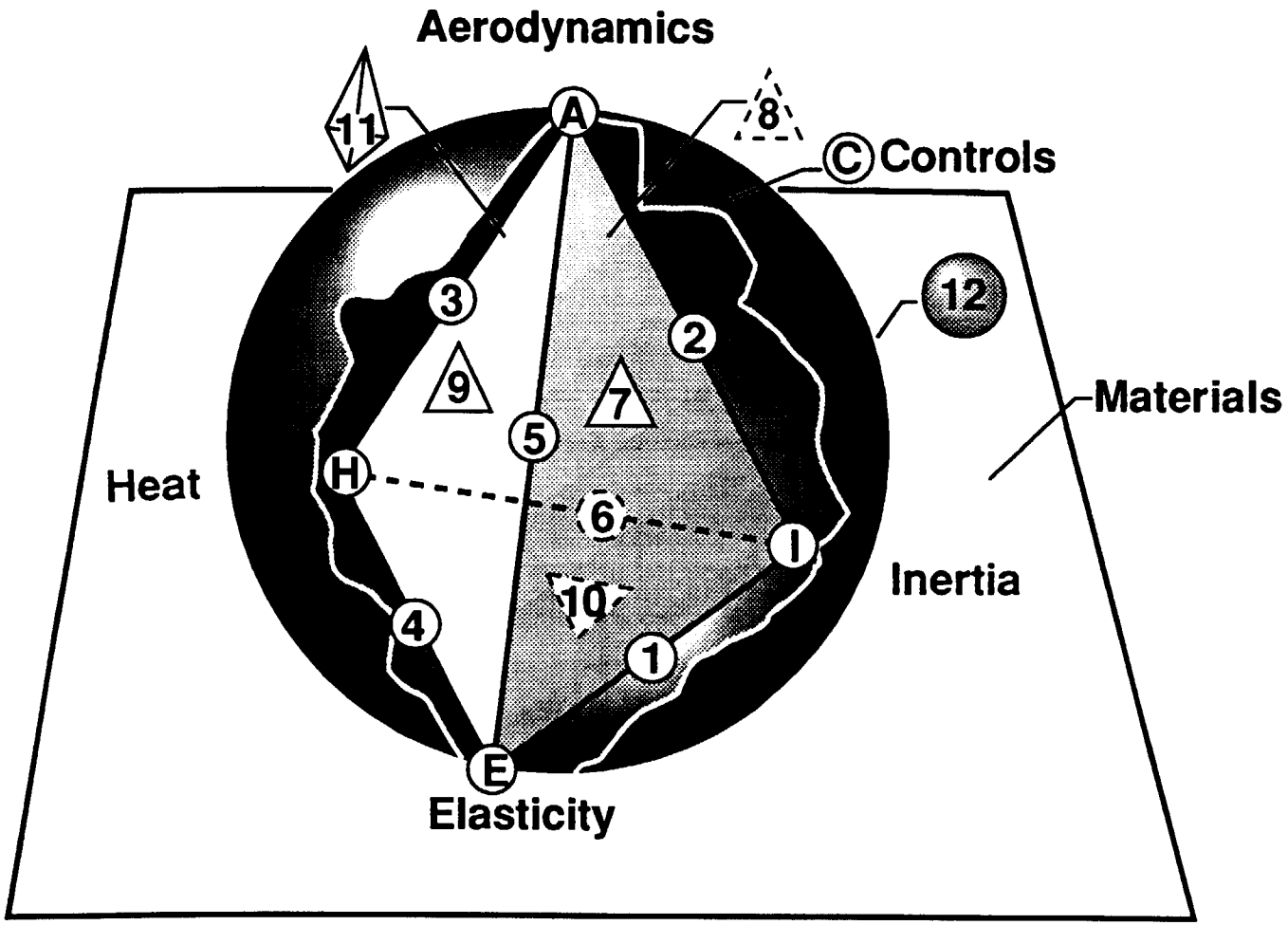

1 Vibration
2 Stability
3 Aerothermodynamics
4 Thermoelasticity
5 Aeroelasticity, static
6 Thermal molecular processes
7 Aeroelasticity, dynamic
8 Stability and heat
9 Aerothermoelasticity, static
10 Vibration and heat
11 Aerothermoelasticity, dynamic
12 Aeroservothermoelasticity

Figure 2. - Aeroservothermoelasticity spheroid.

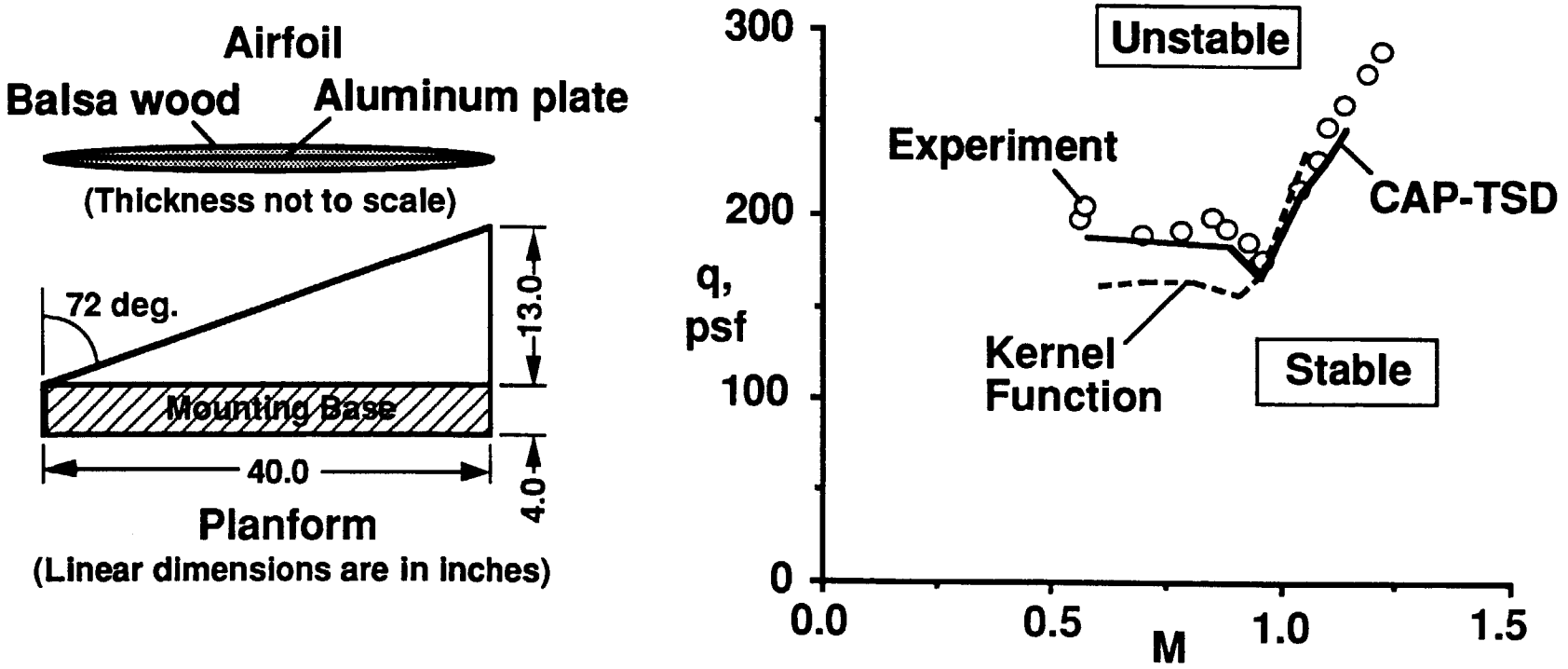

Figure 3. - Experimental and analytical flutter results for 72°-swept delta-wing model.

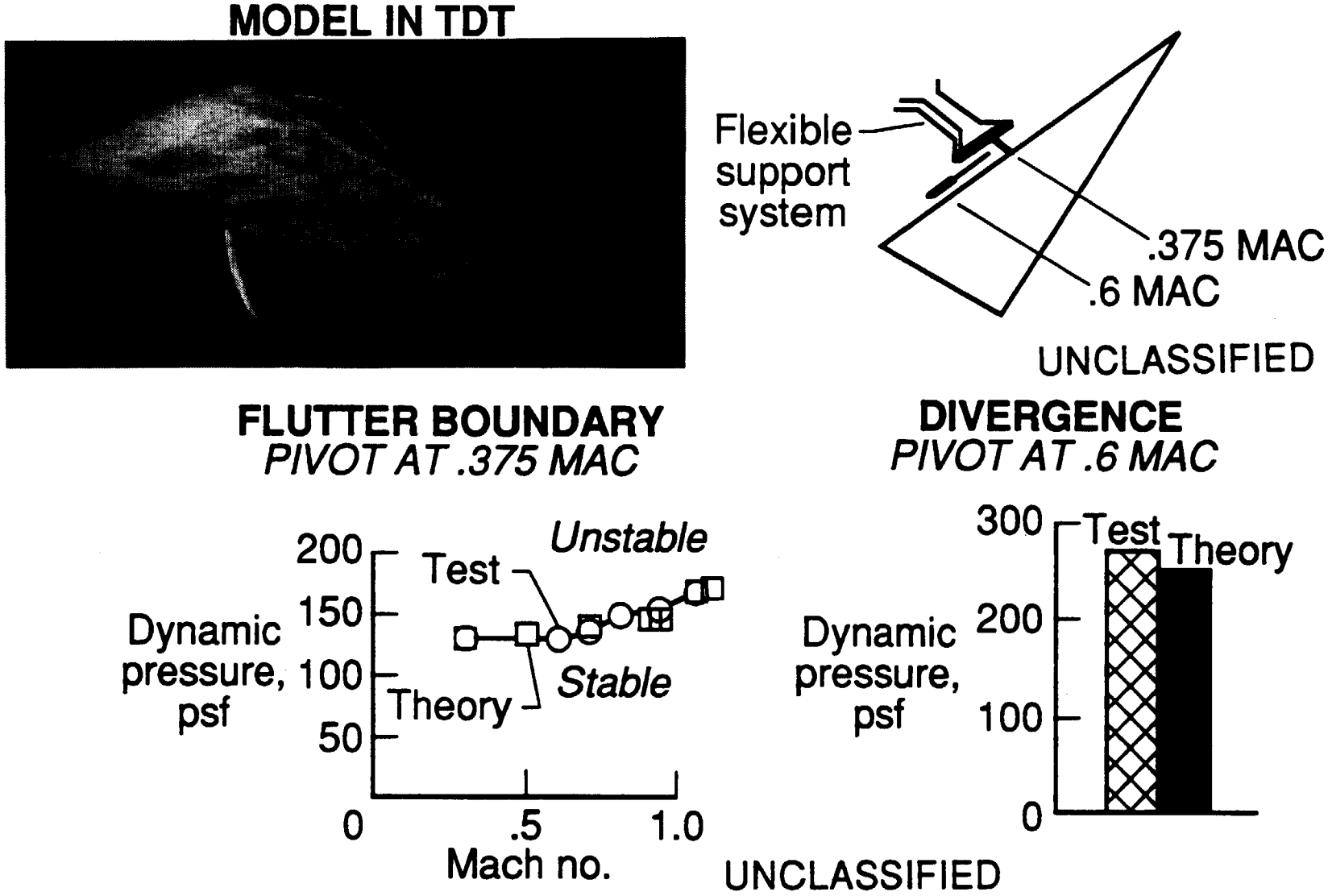

Figure 4. - Experimental and analytical flutter and divergence results for all-moveable delta-wing model.

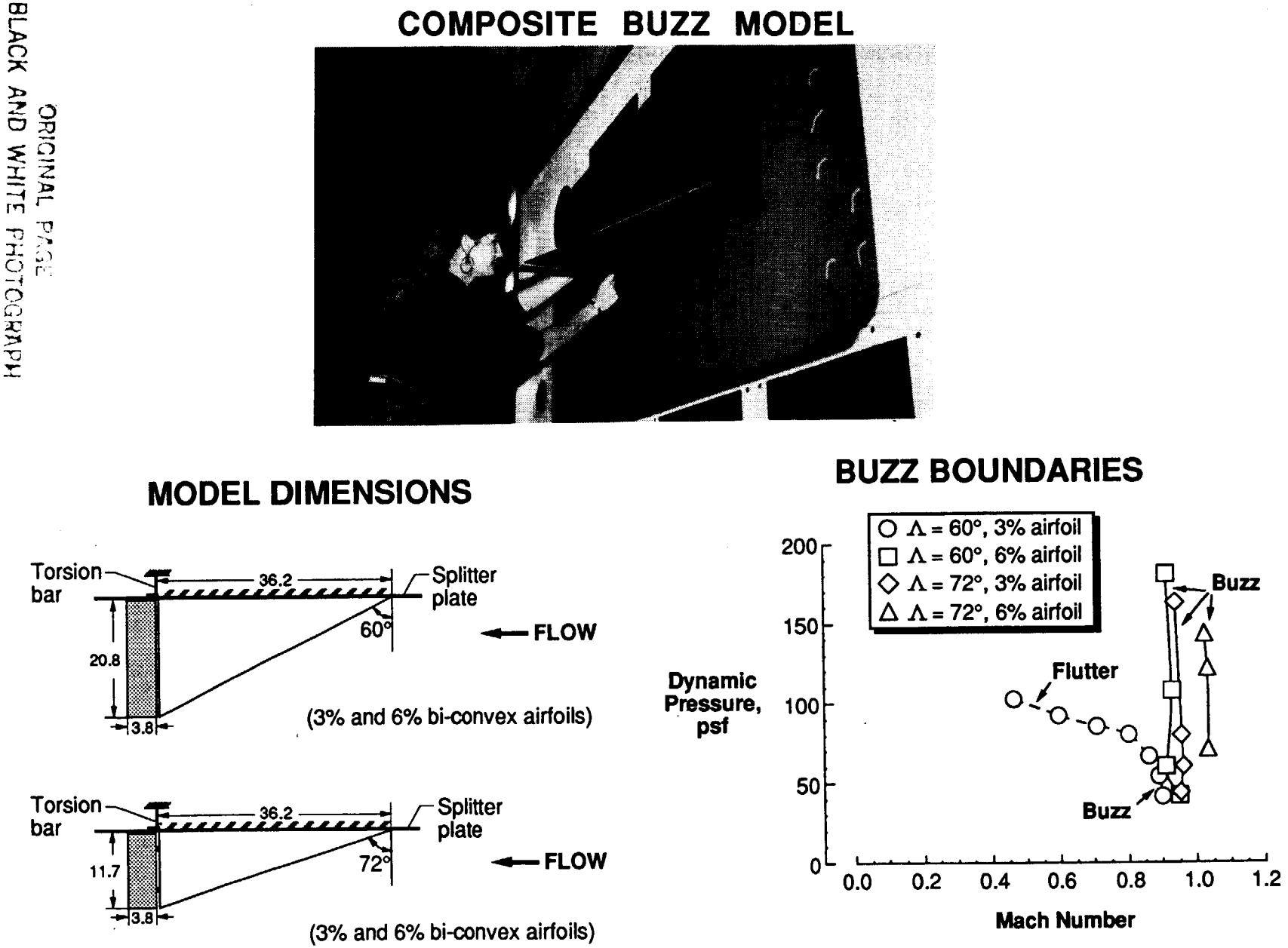

Figure 5. - Effects of leading-edge sweep and airfoil thickness on control-surface buzz.

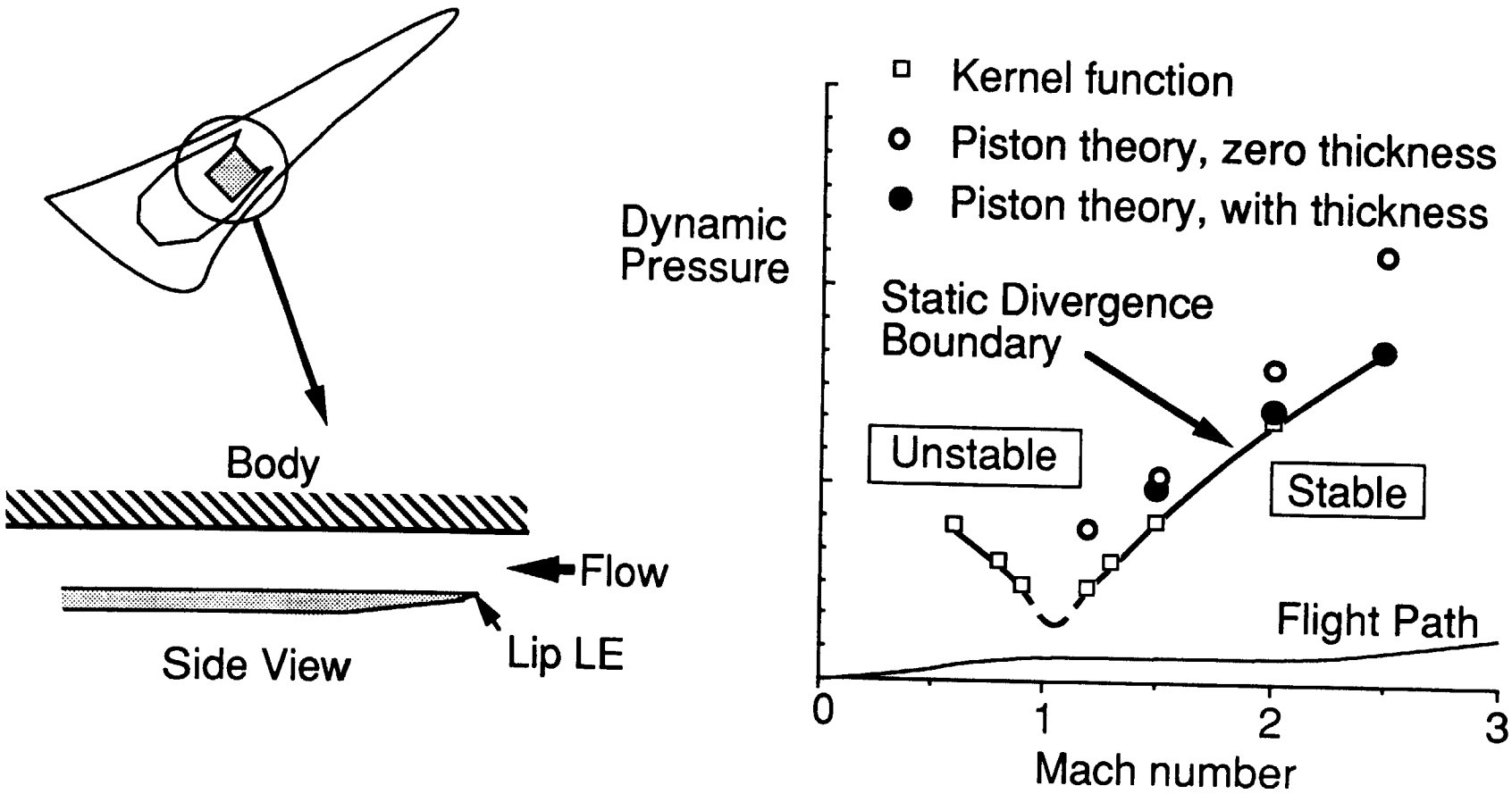

Figure 6. - Calculated divergence boundaries for engine inlet lip.

-New FPE finite-volume formulation completed
-FPE method permits use of body-fitted grids
-2D method coded to demonstrate capability

NACA 0012 Airfoil at M=0.75, α=2°

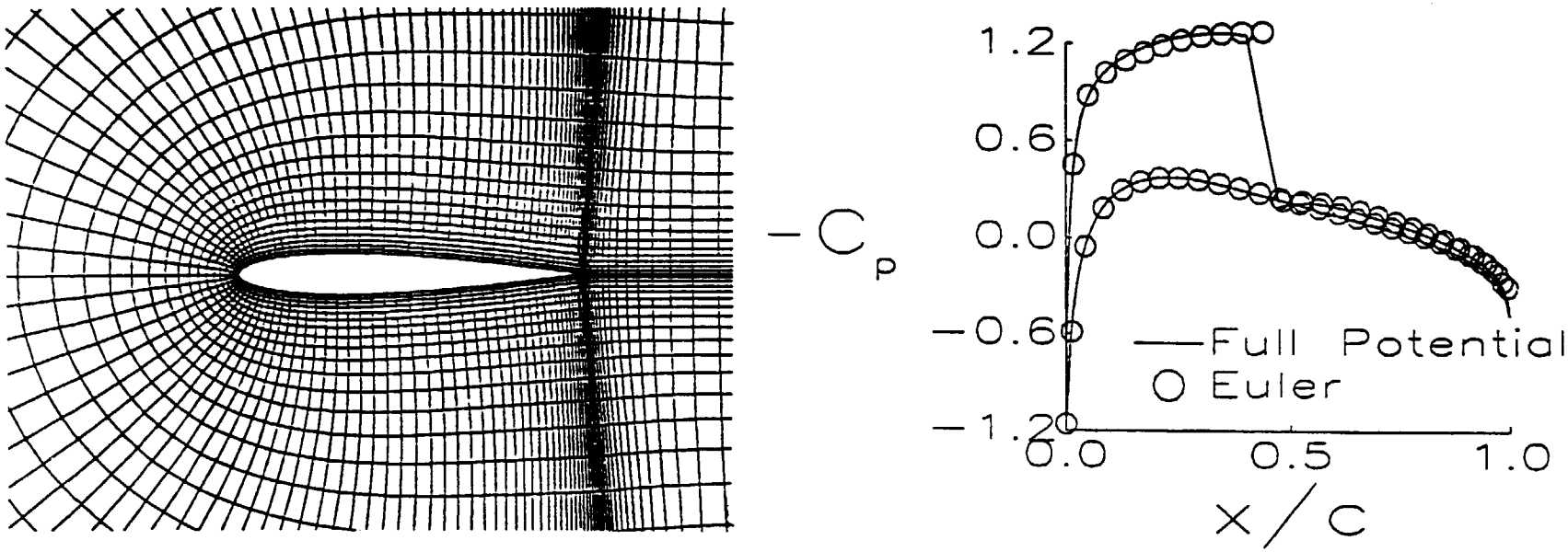

Figure 7. - Illustrative two-dimensional results using full-potential-flow equation method.

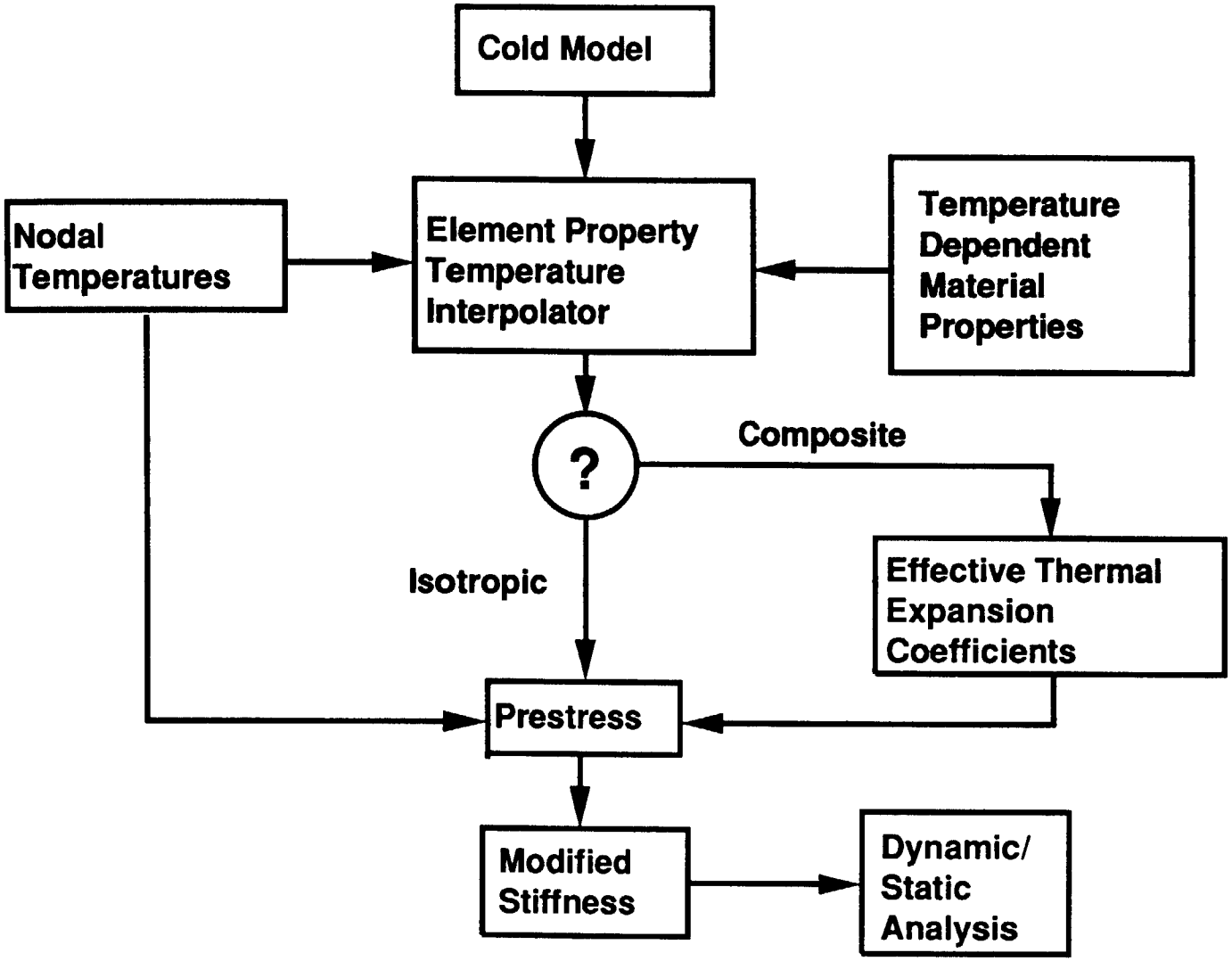

Figure 8. - Process for including thermal effects into finite-element analysis.

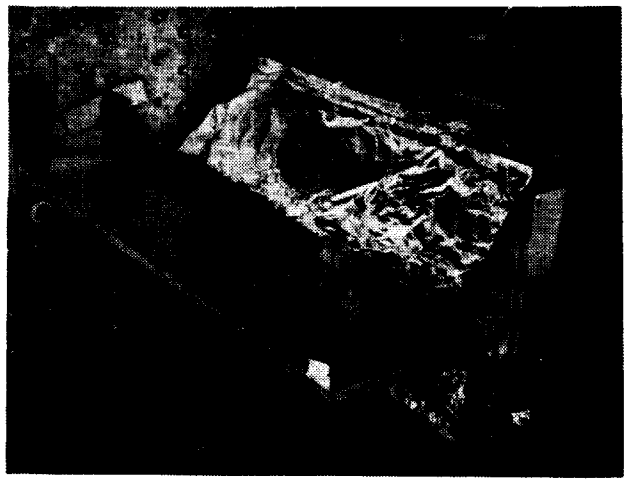

Test arrangement

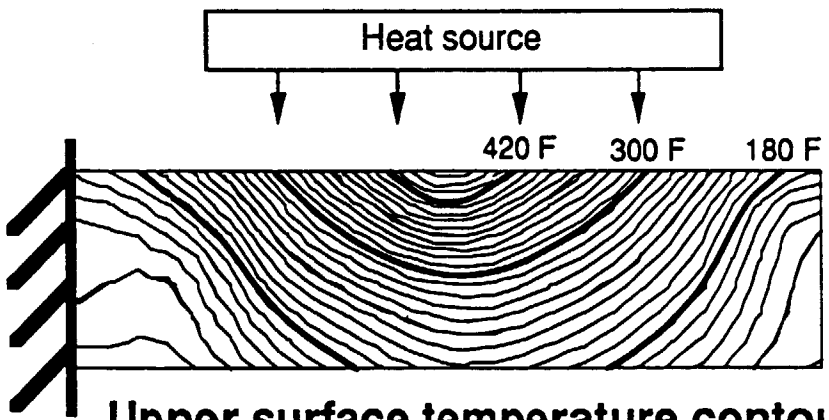

Upper surface temperature contour at hottest condition

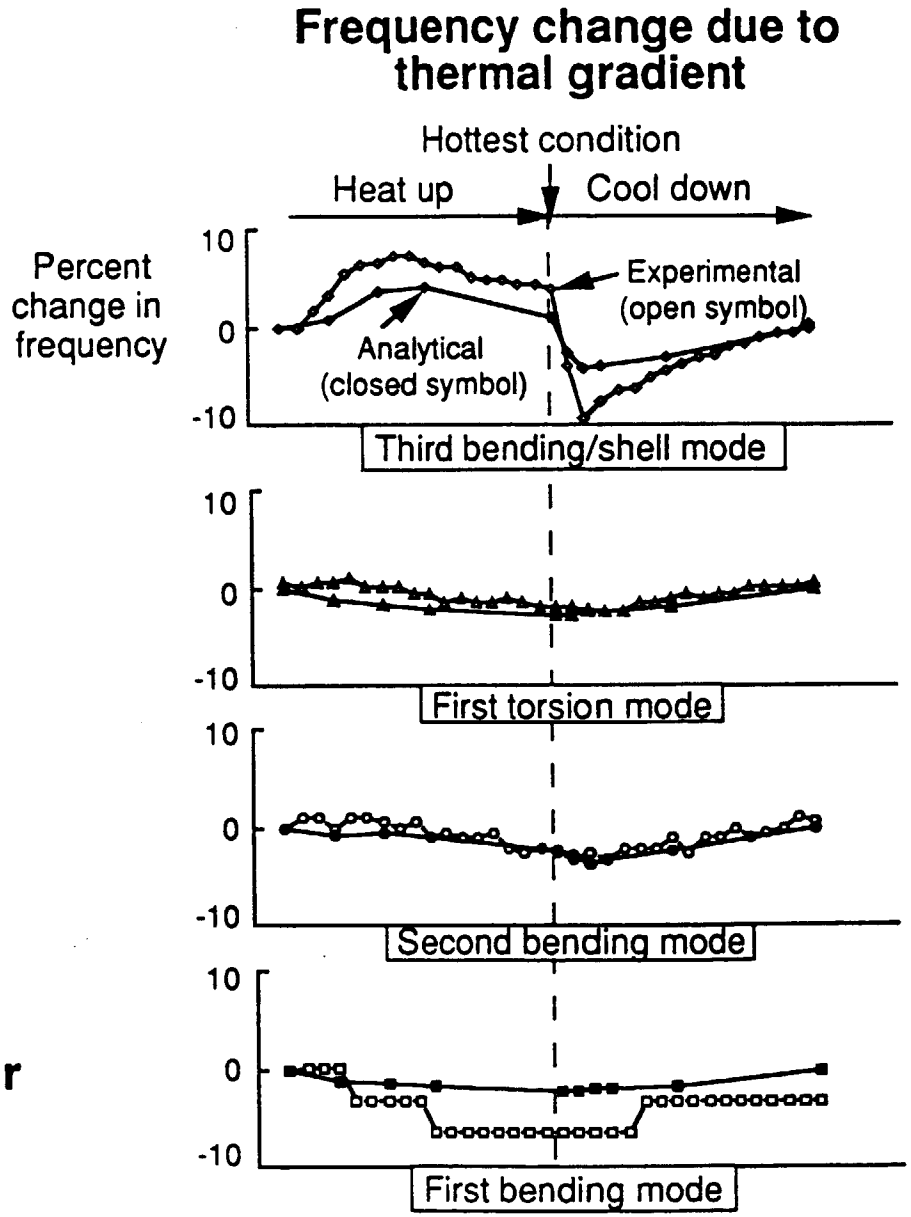

Figure 9. - Calculated and measured thermal effects on natural vibration frequencies.

WIND-TUNNEL MODEL

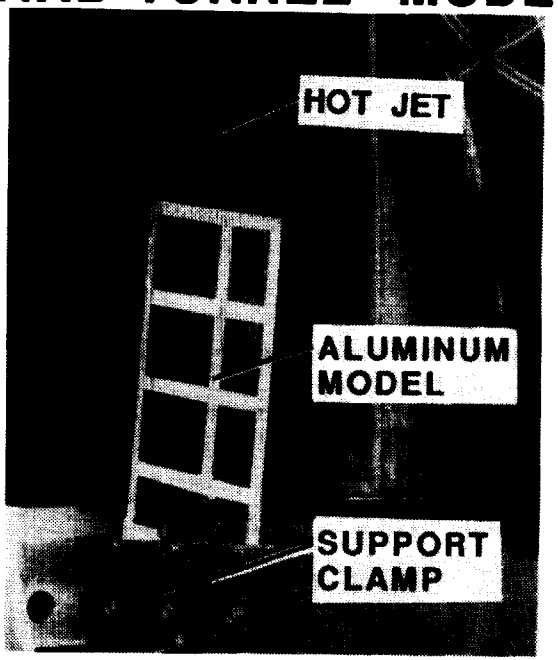

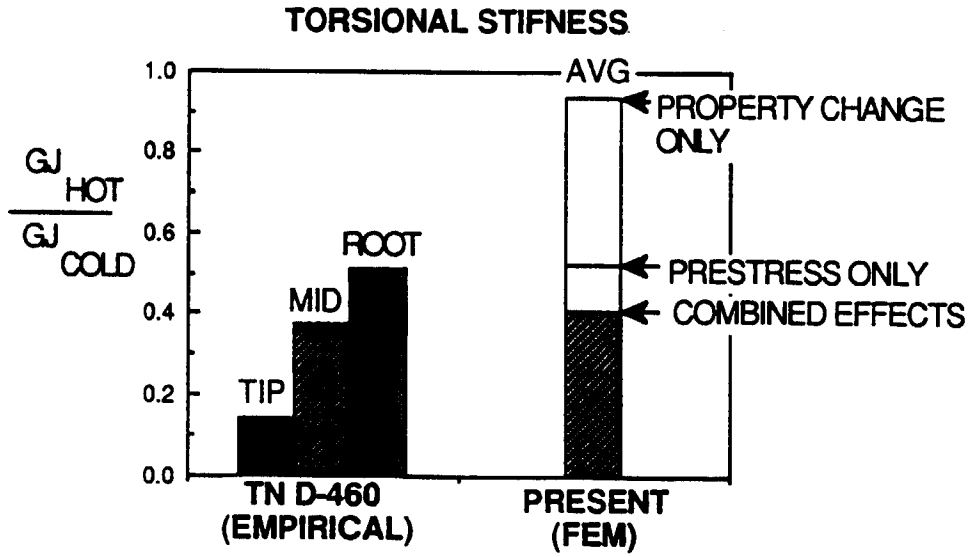

FLUTTER

Flutter due to transient temperature distribution occurring 2 seconds after start at Mach 2 in 800°F air.

$$q_{exp} = 6895 \text{ psf}; \quad q_{FEM} = 7445 \text{ psf}.$$

FEM method also includes piston theory unsteady aerodynamics and flutter solution method (STABCAR).

Figure 10. - Comparison of calculated and measured stiffness and flutter speeds of heated model.

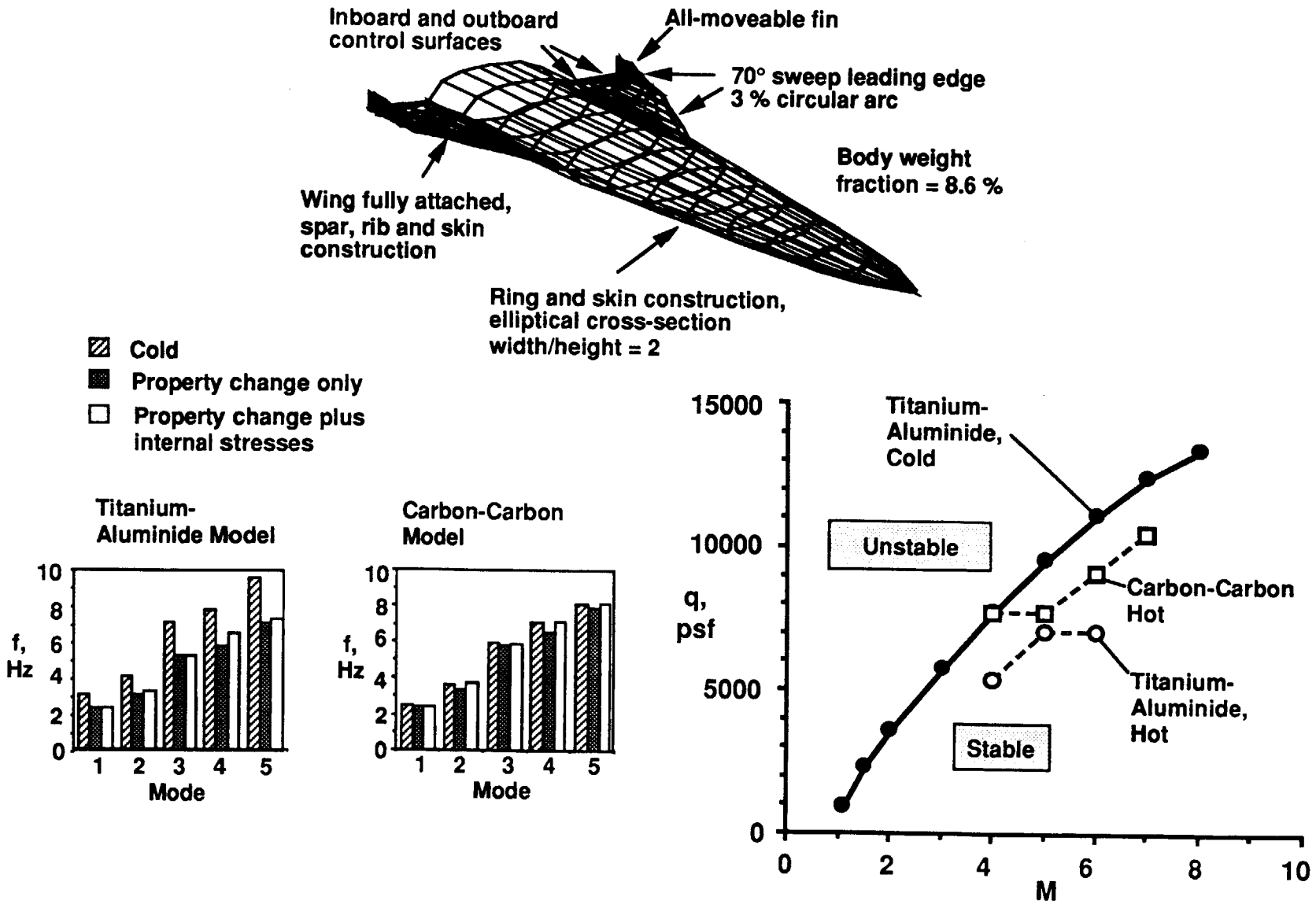

Figure 11. - Calculated effects of heating on the flutter characteristics of a generic NASP design.

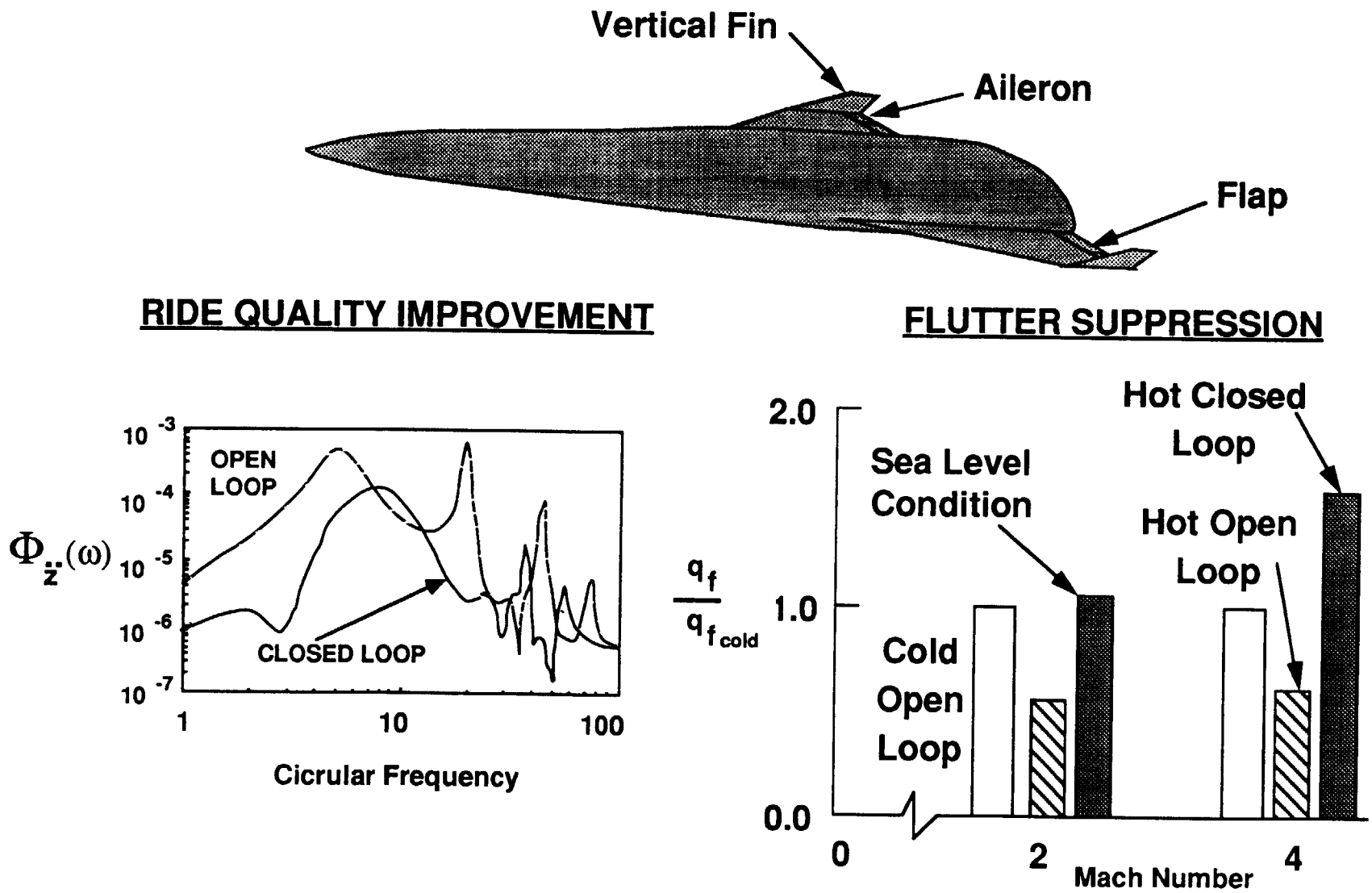

Figure 12. - Active flutter suppression and ride quality improvement for a generic NASP design.

NASA
National Aeronautics and Space Administration

Report Documentation Page

1. Report No.	2. Government Accession No.	3. Recipient's Catalog No.
NASA TM-104058		

4. Title and Subtitle	5. Report Date
NASP Aeroservothermoelasticity Studies	April 1991
	6. Performing Organization Code

7. Author(s)	8. Performing Organization Report No.
Robert V. Doggett, Jr., Rodney H. Ricketts, T. E. Noll, and John B. Malone	
	10. Work Unit No. 763-23-41-71

9. Performing Organization Name and Address	11. Contract or Grant No.
NASA Langley Research Center Hampton, VA 23665-5225	
	13. Type of Report and Period Covered

12. Sponsoring Agency Name and Address	Technical Memorandum
National Aeronautics and Space Administration Washington, DC 20546-0001	14. Sponsoring Agency Code

15. Supplementary Notes

This report is similar to the report "NASP Aerothermoelasticity - A Review, " paper no. 104, Tenth National Aero-Space Plane Technology Symposium, April 23-26, 1991. The report is reissued in the present expanded form to provide a boarder dissemination of the information.

16. Abstract

Some illustrative results obtained from work accomplished under the Aerothermoelasticity work breakdown structure (WBS) element (4.7.02) of the National Aero-Space Plane (NASP) Technology Maturation Program (TMP) are presented and discussed. The objectives of the Aerothermoelasticity element were to develop analytical methods applicable to aerospace plane type configurations, to conduct analytical studies to identify potential problems and to evaluate potential solutions to said problems, and to provide an experimental data base to verify codes and analytical trends. Work accomplished in the three areas of experimental data base, unsteady aerodynamics, and integrated analysis methodology are described. Some of the specific topics discussed are transonic wind-tunnel aeroelastic model tests of cantilever delta-wing models, of an all-moveable delta-wing model, and of aileron buzz models; unsteady aerodynamic theory correlation with experiment and theory improvements; and integrated analysis methodology results for thermal effects on vibration, for thermal effects on flutter, and for improving aeroelastic performance by using active controls.

17. Key Words (Suggested by Author(s))	18. Distribution Statement
Aeroelasticity Aeroservoelasticity Aerothermoelasticity Aeroservothermoelasticity	Unclassified - Unlimited Subject Category 02

19. Security Classif. (of this report)	20. Security Classif. (of this page)	21. No. of pages	22. Price
Unclassified	Unclassified	25	A03